ORIGINAL PAPER

Study on High and Steep Slope Stability and Slope Angle Optimization of Open-Pit Based on Limit Equilibrium and Numerical Simulation

Yaodong Zhou · ping Zou · Feifei Wang · Zhengyu Liu · Wanjie Hu · Zeng Ma

Abstract The stability of open-pit slope is related to mine safety, especially for high and steep slope. In order to obtain the design slope stability and slope angle optimization of K mine open-pit in Myanmar, limit equilibrium analysis method and three-dimensional numerical simulation are used to carry out the study on the slope stability. The results show that: (1) The safety factor of the designed slope is larger than the allowable safety factor by using the limit equilibrium analysis, which belongs to the stable slope. Some areas can be optimized for design. (2) Through three-dimensional numerical analysis, the design slope and the optimized slope are both stable. The area with large deformation of the optimized slope is mainly concentrated in the area of 562 m level moderately weathered pyroclastic rock in area A and 560 m level moderately weathered rock in area B. The calculation results of three-dimensional numerical simulation are basically consistent with the results of the limit equilibrium analysis. (3) Compared with the designed slope, the potential sliding surface position of the optimized slope is lower. The safety factor is smaller, but larger than the allowable safety factor. The shape of the sliding surface of the whole slope is nearly circular arc. The sliding mode of the slope is circular arc sliding. (4) The reasonable slope angle of different engineering geological divisions of the open-pit slope of K mine is determined. The overall slope angle of area A is $\leq 46°$. The overall slope angle of area B is $\leq 44°$. The overall slope angle of area C is $\leq 45°$. The overall slope angle of area D is $\leq 50°$. The research results can provide reference for mine safety production.

Keywords Mining engineering · Slope engineering · Open pit slope · Numerical simulation · Slope stability

Y. Zhou
Wanbao Ming Ltd., Beijing 100053, China

p. Zou · F. Wang (✉) · Z. Liu · W. Hu · Z. Ma
State key Laboratory of Safety Technology of Metal Mines, Changsha 410012, Hunan, China
e-mail: 1942016362@qq.com

p. Zou · F. Wang · Z. Liu · W. Hu · Z. Ma
Changsha Institute of Mining Research Co., Ltd, Changsha 410012, Hunan, China

F. Wang
School of Civil Engineering, Chongqing Jiaotong University, Chongqing 400074, China

1 Introduction

Since the twentieth century, the proportion of open-pit mining at home and abroad has been increasing. In recent years, with the rapid development of industry, the demand for mineral resources is growing. Most of the open-pit mines turn to deep mining and begin to develop and utilize the deep open-pit mines. In the mining process of deep open-pit mine, the slope

stability is getting worse with the increase of mining depth (Yang et al., 2011). On the premise of ensuring safety, improving the slope angle has a great impact on the economic benefits of the mine. In the mining process of deep open-pit mine, slope stability analysis and optimization design are of great significance to ensure safe production and improve economic benefits (Hu et al., 2011).

At present, Scholars have carried out a lot of research on slope stability analysis methods and applications (Duncan and Wright 1980; Hovland et al., 1977; Hungr et al., 1987; Huang and Tsai 2000; Chen et al., 2001). Some scholars have carried out the study on the optimization of slope structural parameters of open pit. The optimized slope can not only ensure the slope stability, but also achieve the maximum economic benefits. The production life of a mine has been extended (Pan et al., 2017; Guan et al., 2018; Han and Lu 2018; Zou et al., 2016).

Cao et al. (2018) studied the deformation and failure mechanism and stability of the high and steep slope systematically by using the Morgenstern price limit equilibrium method and the finite element numerical simulation software RFPA, based on the engineering background of the high and steep slope in the deformation area of the south side of Fushun West open-pit mine. Liu et al. (2017) took the west-I area of Luming molybdenum mine as the main research background, according to the engineering geological conditions and mining design scheme of the slope in the west-I area of Luming molybdenum mine, established the numerical simulation mechanical model for the three selected sections in the west-I area, analyzed and calculated the safety coefficient of the slope using the geo slope software based on the limit equilibrium method, and evaluated the slope stability. Wang et al. (2009) proposed a new three-dimensional calculation method for the stability of concave slope based on the limit equilibrium theory and quantitative understanding of the earth's circumferential lateral pressure. The accuracy of this method is verified by comparing it with the classical three-dimensional limit equilibrium method.

Deng and Liliang (2012) established the hypothesis of the inter slice force corresponding to the horizontal and vertical slice methods by studying the relationship between the inter slice forces in horizontal and vertical slice methods. The safety factor formulas of Swedish method, simplified Bishop method, simplified Janbu

method and morgenster price (M-P) method in horizontal slice time are derived. Jyant and Pijiush (2006) proposed a method to calculate the stability number of layered soil slope by using the upper bound analysis method. The fracture surface is assumed to be a combination of different logarithmic spiral arcs with a common focus. Through the analysis of the slope stability research carried out by the above scholars, abundant research results have been achieved in the slope stability research. There is no systematic study on the stability of open-pit slope under the condition of large scale, high and steep slope.

In this paper, based on the research background of K mine open-pit slope in Myanmar, limit equilibrium and three-dimensional numerical simulation are used

Fig. 1 The location of the phosphate mine

to study the stability and slope angle optimization of high and steep slope. The innovation of this paper is as follows. (1) The stability of open pit slope is analyzed by limit equilibrium and three-dimensional numerical simulation. (2) The optimization of slope structure parameters in open pit is studied. On the premise of ensuring the slope stability, the slope angle is improved. The research results can provide basis for mine safety production and optimization design.

2 General Situation of Mine

2.1 Geologic Strata

The K mine of Monyova copper mine is located in the south of Sagaing Province in the northwest of the union of Myanmar (see Fig. 1). The K mine belongs to kyisintaung ore section of Monyova copper deposit. The exposed strata in the mining area are generally simple, mainly composed of Paleogene Oligocene damapala formation sandstone and quartz sandstone, Miocene Pliocene majigan formation volcaniclastic rock and sandstone, quaternary Pleistocene kangang formation siltstone, argillaceous sandstone, quaternary Holocene eluvium and diluvium, and Miocene intrusive magmatic rock.

The relationship between lithology, thickness, rock characteristics, rock equality and mineral distribution of each layer is described as follows.

(1) Paleogene Oligocene damapala formation.

It is mainly concentrated in the deep part of the South and South West of the mining pit in the mining
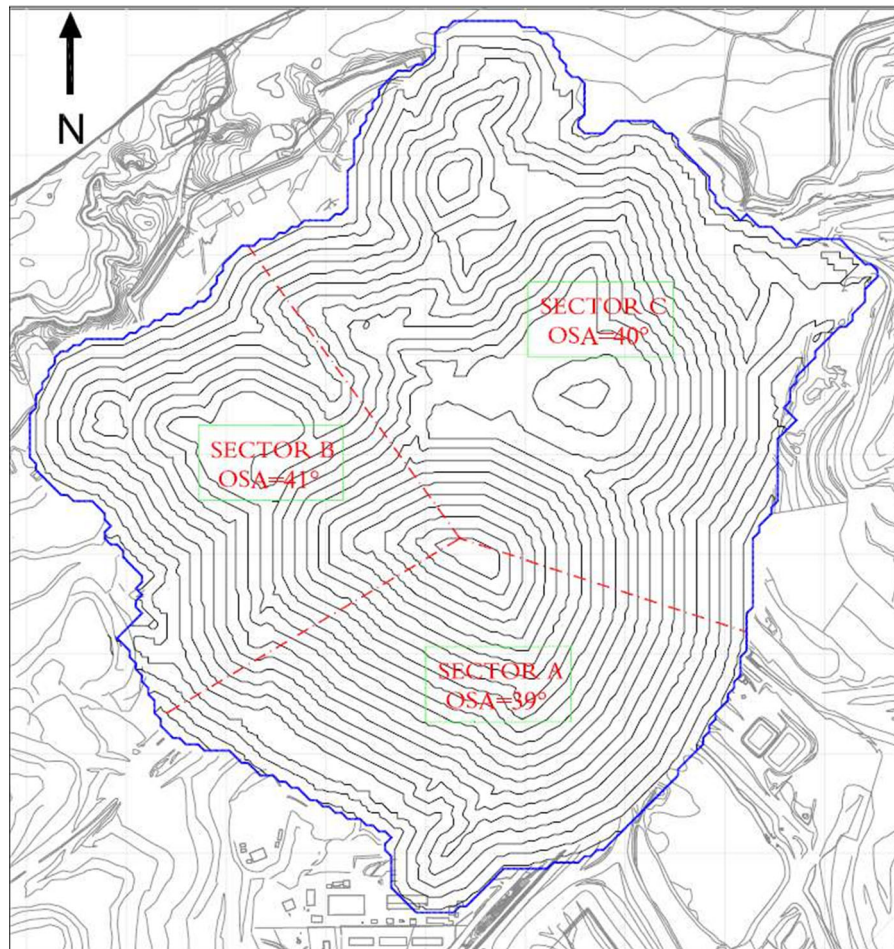

Fig. 2 Recommended slope angle zoning map of K-mine

area, and the surface is not exposed, which is exposed by drilling engineering. The exposed elevation is 619.60∼254.00 m, and the exposed thickness is 2.28∼114.58 m. It inclines to the northeast with a dip angle of 10∼25°. It is an integrated contact with the overlying strata.

(2) Miocene Pliocene majigang formation of Neogene.

It is mainly distributed in the southeast, the upper part of the southwest and the surrounding of the mining area. The lithology is mainly volcanic clastic rock, sandstone and siltstone. The pyroclastic rocks are gray, purple gray, brownish yellow after weathering, with volcanic breccia structure and massive structure. The thickness is 185∼292 m, which is in integrated contact with the underlying strata, and in fault contact with the andesite porphyry (andesite porphyry) in the mining area.

(3) Quaternary Pleistocene kanggang formation.

It is mainly distributed around the mining area K and at the foot of the hill. The thickness is about 40 m. The dip angle is less than 25°.

(4) Quaternary Holocene.

The Quaternary sediments in the mining area are mainly alluvial proluvial and eluvial Deluvial, which are distributed in the northwest of the mining area near the yama river.

2.2 Ore Body Characteristics

The continuous ore body is the main ore body of K mine and a complete ore body with large thickness and good continuity. The distribution elevation of the continuous ore body is -6∼694 m, which is generally in the shape of stratiform and bell emulsion. The
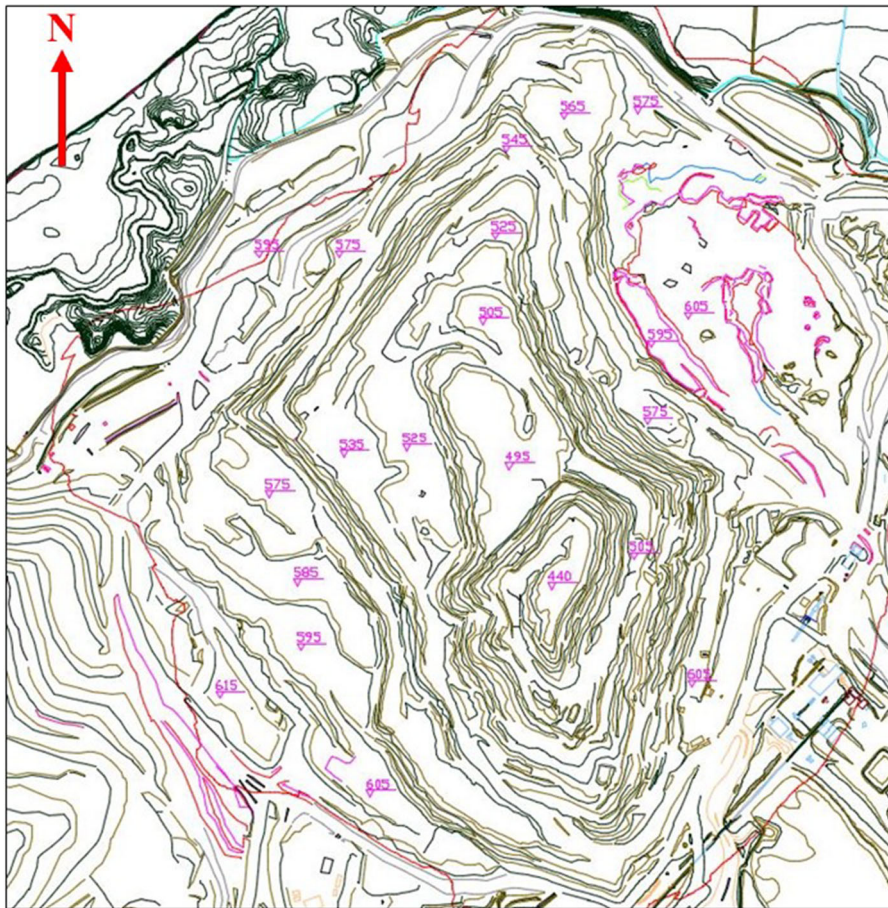

Fig. 3 Current situation of open-pit

length is about 1400 m, and the width is 1000 m. The ore body scale is large. The thickness of the ore body is $4 \sim 628.04$ m, with an average thickness of 108.37 m. Generally, the thickness of the west side of the ore body is obviously thinner than that of the east side. The orebody inclines to the southeast with a dip angle of $40 \sim 60°$. The discontinuous ore body is unevenly distributed at $34 \sim 638$ m elevation and the thickness of ore body is $4.02 \sim 141.15$ m.

2.3 Mining Design

The mining method of K mine is open-pit mining. The designed stope slope parameters are as follows. Step height is 10 m (final parallel section is 20 m). Width of safety platform is 8 m. Width of cleaning platform is 16 m. Width of transportation road is 16 m for single line and 21 m for double line. Maximum gradient of transportation line is 8%. Minimum radius of curve of transportation line is 20 m. Control angles

Table 1 Overview of slopes in each engineering geological division

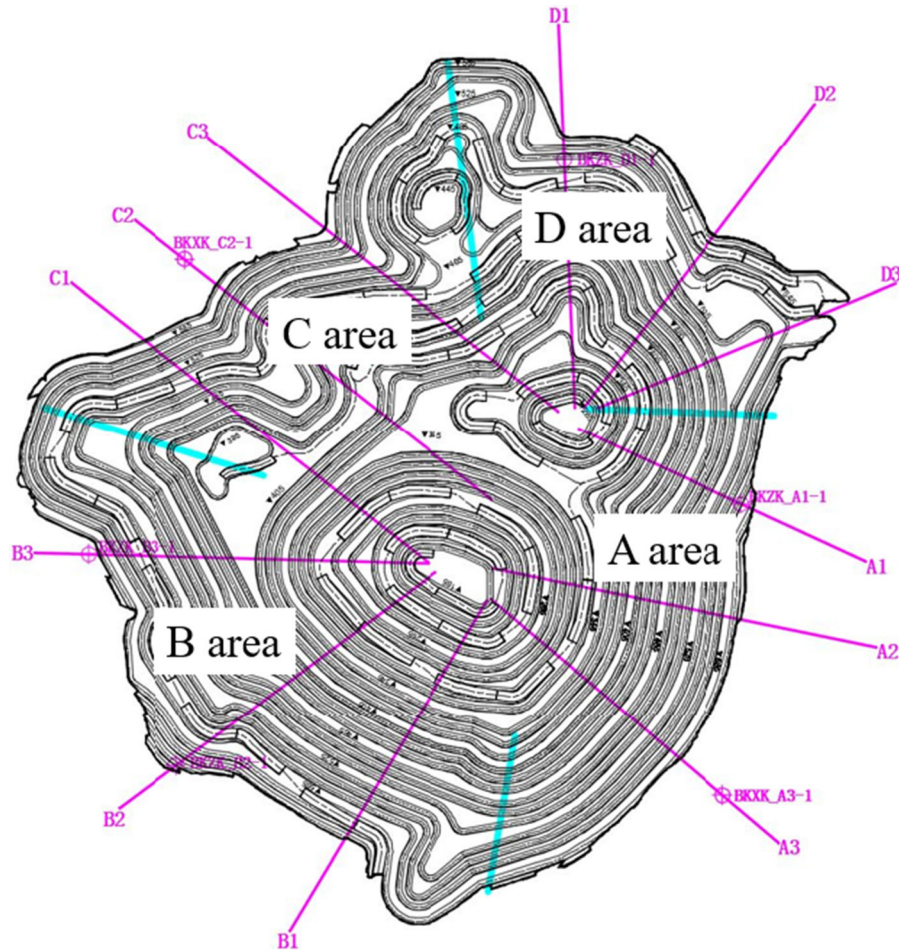| Areas	Level (m)	Maximum slope height (m)	Slope shape
A	$185 \sim 720$	535	Straight line and arc shape
B	$185 \sim 740$	555	
C	$185 \sim 594$	409	
D	$285 \sim 583$	298	

Fig. 4 Engineering geological division and analysis section layout of open pit

Table 3 Slope parameters designed for location of analysis section in each zone

Zone	Section	Designed overall slope angle (°)	Elevation (m)	Maximum design slope height in open boundary (m)	Boundary water level (m)
A	A1	39.4	285~595	310	500.38
	A2	38.3	185~605	420	501.93
	A3	38.9	185~595	410	585.06
B	B1	37.5	185~615	430	593.22
	B2	35.3	185~645	460	603.04
	B3	32.6	185~595	410	588.32
C	C1	29.2	185~585	400	574.31
	C2	24.1	265~585	320	582.61
	C3	26.9	285~585	300	576.32
D	D1	28.1	285~575	290	572.41
	D2	34.4	285~575	290	572.61
	D3	27.5	285~535	250	559.81
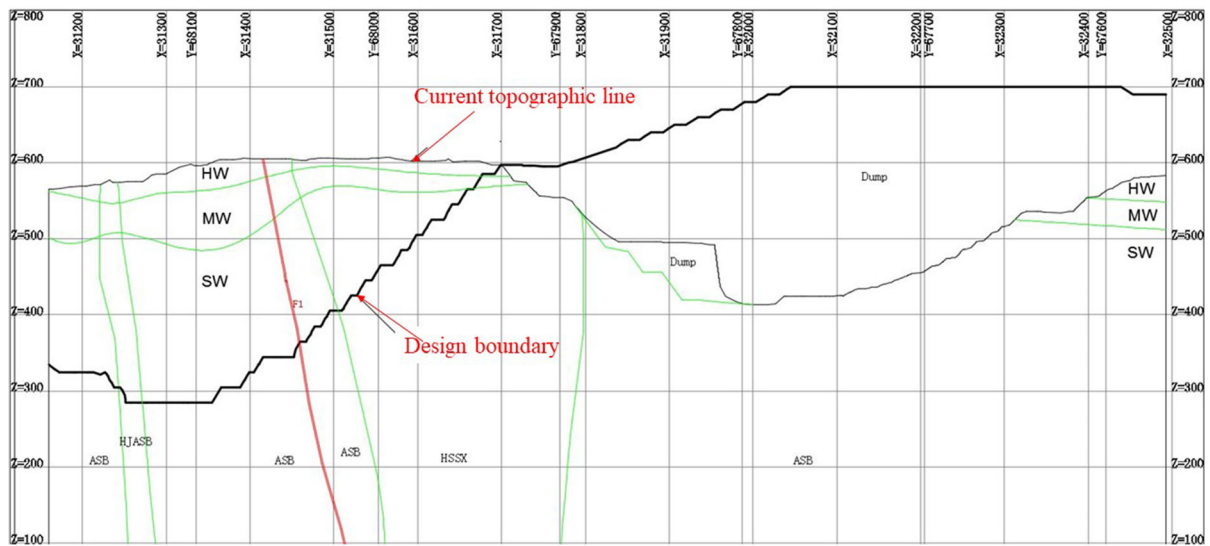
Fig. 5 A1 engineering geological profile

of final slope angle are area A ≤ 39°, area B ≤ 41°, area C ≤ 40° (see Fig. 2). Slope angle of finishing steps is 60° below the 585 m elevation and 55° above the 585 m elevation.

2.4 Mining Status

K mine started construction in 2013. After two years of construction, it was officially put into production in 2015. After several years of production, the mine has formed a mature and perfect mining, beneficiation and smelting system.

Through the construction and production stripping of K mine from 2013 to 2017 years, K mine has formed an open-pit with a growth of 750~980 m and a width of 550~700 m. The maximum mining elevation is 605 m, the minimum mining elevation is 455 m, and the maximum slope height is more than 150 m. From top to bottom, it has been mined into 15 steps. Except that the south side of the stope is close to

Table 4 Rock mass mechanical parameters

Rock types	Density / (g/cm^3)	Elastic Modulus E/(MPa)	Poisson Ratio μ	Cohesion C/(MPa)	Angle of Internal Friction φ/(°)
Strongly weathered andesite porphyry	2.23	241.83	0.30	0.16	24
Moderately weathered andesite porphyry	2.39	1561.44	0.30	0.25	32
Slightly weathered andesite porphyry	2.58	3587.58	0.22	0.76	37
Strongly weathered pyroclastic rock	2.15	284.52	0.29	0.17	25
Moderately weathered volcanic clastic rock	2.26	1060.40	0.23	0.20	30
Slightly weathered pyroclastic rock	2.43	4062.90	0.29	0.67	36
Moderately weathered biotite hornblende mountain porphyry	2.56	2953.59	0.25	0.60	34
Slightly weathered biotite hornblende mountain porphyry	2.64	7884.14	0.22	1.10	39
Slightly weathered sandstone	2.59	4010.65	0.20	0.70	35
Quaternary soil	1.96	6	—	0.036	11.41
Waste rock of waste dump	1.91	750	0.29	0.035	32

Table 5 Preliminary design slope stability safety factor results

Sections	Overall slope angle (°)	Analysis method	Condition I	Condition II	Condition III	Condition IV
A1	39.4	B	1.706	1.432	1.366	1.705
		M-P	1.707	1.439	1.378	1.706
A2	38.4	B	1.554	1.321	1.266	1.378
		M-P	1.557	1.330	1.272	1.382
A3	39.1	B	1.524	1.294	1.241	1.350
		M-P	1.525	1301	1.248	1.352
B1	38.8	B	1.509	1.282	1.230	1.356
		M-P	1.507	1.289	1.235	1.357
B2	39.3	B	1.557	1.313	1.258	1.350
		M-P	1.567	1.331	1.278	1.363
B3	33.7	B	1.594	1.323	1.267	1.430
		M-P	1.599	1.326	1.282	1.442
C1	30.7	B	1.958	1.578	1.505	1.854
		M-P	1.957	1.583	1.510	1.853
C2	24.5	B	2.398	1.868	1.776	2.275
		M-P	2.399	1.876	1.783	2.276
C3	28.7	B	2.211	1.778	1.691	2.023
		M-P	2.208	1.781	1.695	2.021
D1	28.9	B	2.160	1.742	1.659	2.016
		M-P	2.160	1.749	1.666	2.016
D2	34.2	B	1.910	1.602	1.529	1.721
		M-P	1.906	1.610	1.538	1.722
D3	30.0	B	1.982	1.676	1.600	1.880
		M-P	1.981	1.678	1.610	1.881

Table 6 Summary of slope angle results of each analysis and calculation section in each zone

Area	Sections	Slope angle (°)	
		Each slope	Each area
A	A1	46	46
	A2	47	
	A3	46	
B	B1	44	44
	B2	45	
	B3	45	
C	C1	45	45
	C2	45	
	C3	45	
D	D1	50	50
	D2	50	
	D3	51	

the boundary edge, the rest of the stope slope is not close to the side, which is a temporary slope. The height of the production step is 10 m, and part of the area is 20 m. In the east side of the slope, a 35 m high slope is formed due to collapse. The width of the safety platform and the cleaning platform is 10 m, and the slope angle of the current slope step is about 65°.

By the end of February 2019, among the steps formed in the open-pit of K mine, the highest elevation is 615 m (south slope, side by side), the lowest elevation is about 440 m (waste water pool in the south of the pit), and the maximum depression slope height is about 175 m. At present, mining and stripping operations are mainly concentrated on the South and north slopes.

3 Limit Equilibrium Analysis

3.1 Theoretical Basis

The limit equilibrium analysis methods mainly include Fellenius method, simplified Bishop method, Janbu simplified method, Spencer method, Morgen Prince method, etc. It is divided into many methods according to the shape of the slope slip surface and the assumption of the force between the blocks. Because the safety factor value of circular failure of slope calculated by the simplified Bishop method can reflect the actual state of slope stability, which has the

Fig. 6 Stability analysis diagram of safety factor of section B3▶ in preliminary design

advantages of fast calculation speed and reliable results, and is adopted by the majority of scientific and technological personnel, it is the main method of this stability study and evaluation.

(1) simplified Bishop method.

This method assumes that the force between the slits keeps the horizontal direction, that is, it assumes only the horizontal thrust, and does not consider the vertical shear force between the slits. The stability safety factor of circular sliding surface is K.

$$K = \frac{\sum\limits_{i}\left[c_iL_i + (W_i\sec\alpha_i - U_iL_i)\right]\frac{1}{1+\tan\varphi_i\tan\alpha_i/K}}{\sum\limits_{i}(W_i\sin\alpha_i + Q_i\cos\alpha_i)} \quad (1)$$

where is the cohesive force of block No.i. is the internal friction angle of block No.i. is the weight of block No.i and the weight of overlying tailings. is the bottom edge length of block No.i. is the horizontal force acting on block No.i. is the angle between the bottom edge of block No.i and the horizontal plane of coordinate axis. is the horizontal force acting on block No.i.

(2) Morgen-Prince method.

Morgen-Prince method assumes that there are normal forces and tangential forces between two adjacent soil strips, and that there is a certain functional relationship between the two forces in the horizontal direction, which can be expressed as formula (2).

$$X = \lambda f(x)E \quad (2)$$

where X is the tangential force between soil strips. E is the normal force between soil strips. λ is constant.

Because (1) contains K on both sides, it needs to be calculated iteratively to get more accurate results, and the convergence is fast. A large number of calculation examples show that the simplified Bishop method is very close to other accurate calculation results and the analysis accuracy is high. In the analysis result, B represents the result of simplified Bishop method. M-P represents the result of Morgen Prince method.
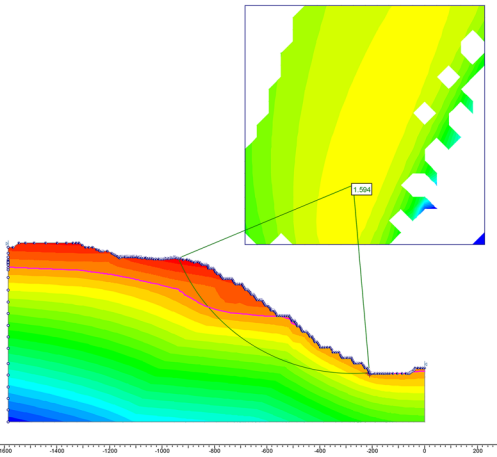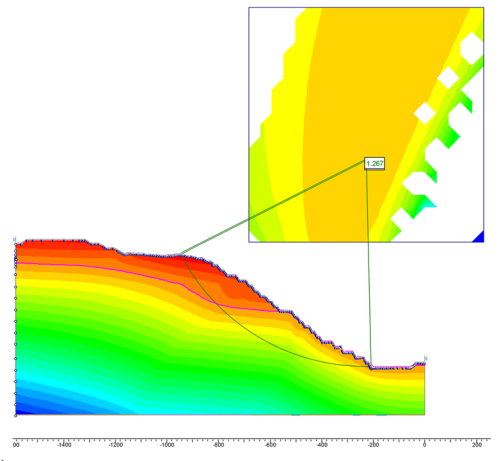
(a) Stability analysis diagram of simplified Bishop method safety factor of section B3 in preliminary design under stress I
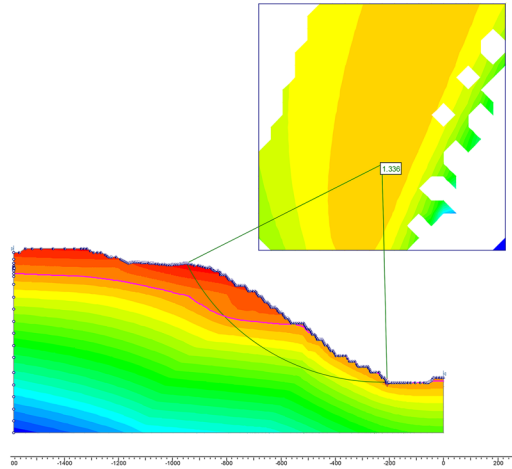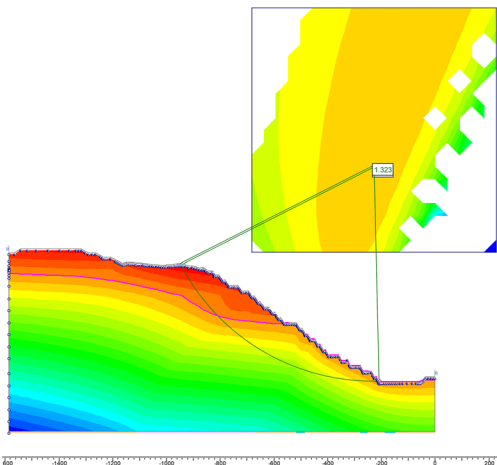

(d) Stability analysis diagram of M-P method safety factor of section B3 in preliminary design under stress II
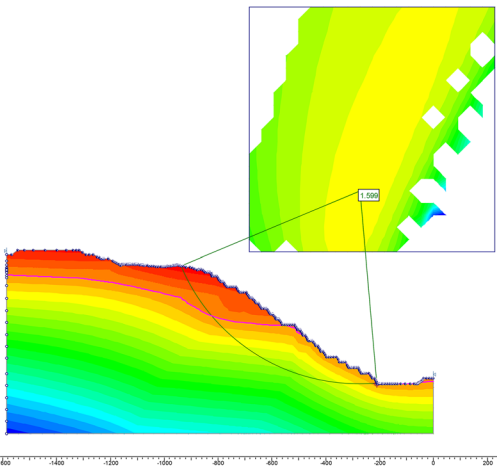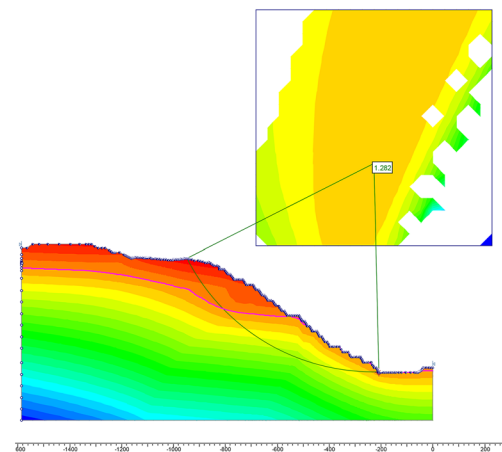

(b) Stability analysis diagram of M-P method safety factor of section B3 in preliminary design under stress I

(e) Stability analysis diagram of simplified Bishop method safety factor of section B3 in preliminary design under stress III

(c) Stability analysis diagram of simplified Bishop method safety factor of section B3 in preliminary design under stress II

(f) Stability analysis diagram of M-P method safety factor of section B3 in preliminary design under stress III

(g) Stability analysis diagram of simplified Bishop method safety factor of section B3 in preliminary design under stress IV
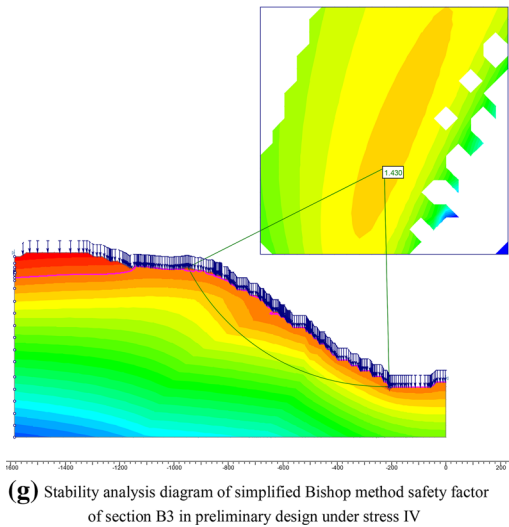
Fig. 6 continued

3.2 Slope Analysis Profile

According to the location and lithology of the slope, the height of the slope, the occurrence of the dominant structural plane of the rock mass and the combination relationship with the slope, the open-pit boundary of K mine is divided into four engineering geological areas. A, B, C and D respectively represent the East, South, West and North areas. The slope profile of each zone is shown in Table 1 and Fig. 4. From Table1, it can be seen that the vertical height of open mining slope in area B is relatively high, about 555 m. The vertical height of open mining slope in area D is relatively low, about 298 m.

The analysis section is the basis of establishing geological model for slope stability study. The layout of the analysis section of open-pit slope stability study is based on the engineering geological division, as shown in Fig. 4, divided into four areas, with a total of 12 sections. The slope parameters designed for the location of each analysis section are shown in Table 3. The A1 engineering geological section is shown in Fig. 5. It can be seen from Table 3 that (1) the slope angle of area C and D is the smallest (24.1 $\sim$ 34.4°). The slope angle between areas A and B is the largest (32.6 $\sim$ 39.4°). (2) In the open-air boundary, the slope height of area B is the largest, and that of area D is the smallest. The slope height of zones A and C is greater than that of area D and less than that of area B.

3.3 Parameter Selection

The rock physical and mechanical test parameters of open mining slope in K mine are treated in engineering. The mechanical parameters of rock mass selected comprehensively are shown in Table 4.

According to code for seismic design of buildings (GB50011-2010) and code for design of non-ferrous metal mining (GB50771-2012), the seismic intensity is VI degree or above, so the impact of earthquake on slope stability shall be studied and analyzed. During the stability analysis of open mining slope of K mine, the local seismic fortification intensity is increased to VIII degree, and the peak acceleration value of ground motion is 0.2 g. Through calculation, the horizontal design seismic acceleration of the mining area is 0.125. Through calculation, the vertical design seismic acceleration of the mining area is 0.0417.

Nubox-8016 vibration intelligent monitor was used to test the blasting vibration of stope, and the statistical and regression analysis were carried out on the test results. The blasting vibration influence coefficient was 0.098 when the distance from the final slope was 60 m.

After slope excavation, groundwater level will gradually decrease with the increase of mining depth. A water level depression funnel is formed in a certain range around the mining pit. But for the sake of safety, the slope is regarded as a large unified water bearing body in the stability analysis. The boundary water level of each section is determined at the periphery of the pit according to the observation water level of the supplementary exploration borehole, the actual water level of the hydrological observation borehole and the contour map of the mining area (see Table 3).

According to the technical code for slope engineering of non-coal open pit mines (GB 51,016–2014) and the characteristics of engineering geology, hydrogeology, slope height and mining service life of open pit slope of K mine, and compared with the open pit mines at home and abroad, the safety grade of K mine slope engineering is grade I, and the allowable safety coefficient [k] under four working conditions is determined.
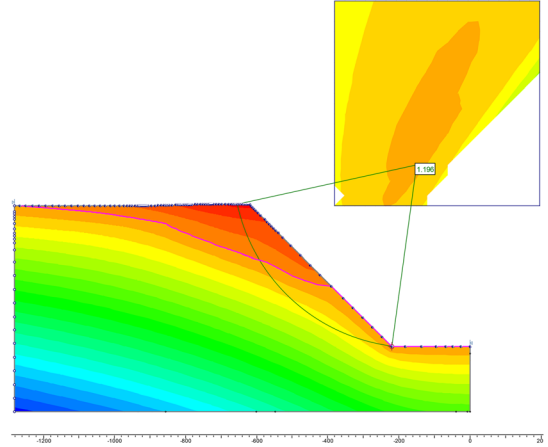
Self weight + groundwater: [k] = 1.25;

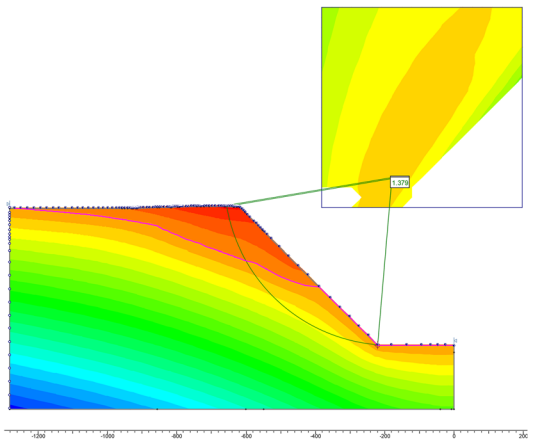Self weight + ground water + blasting vibration force: [k] = 1.18;

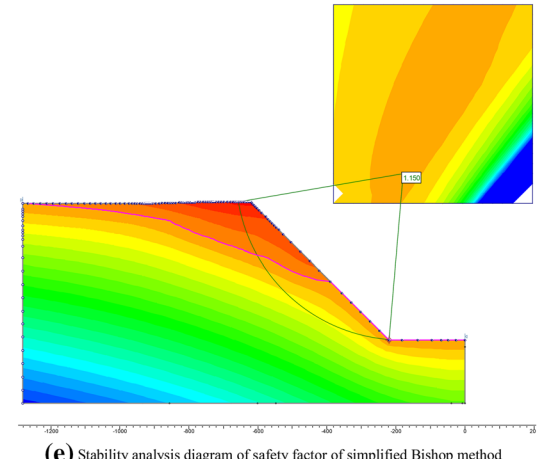Self weight + groundwater + VIII-degree seismic force: [k] = 1.10–1.15;
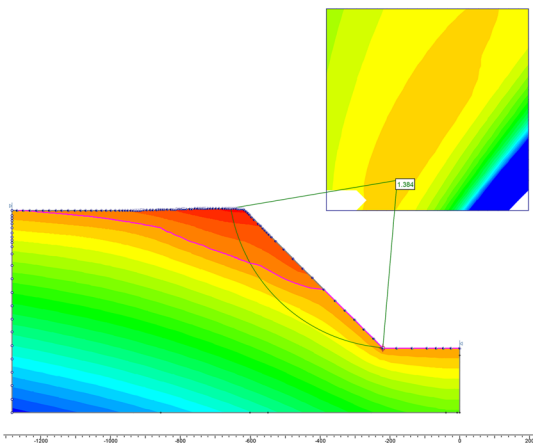
(a) Stability analysis diagram of safety factor of simplified Bishop method for section C2 under 45 ° stress I
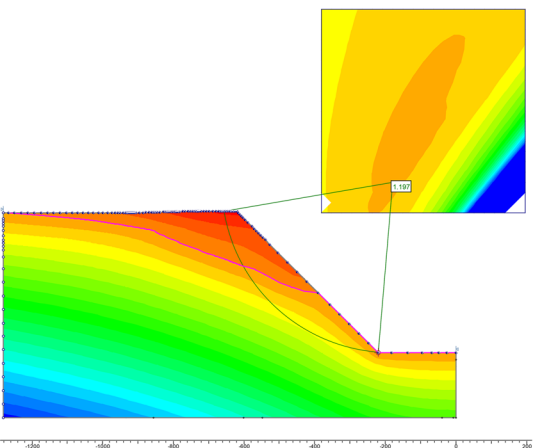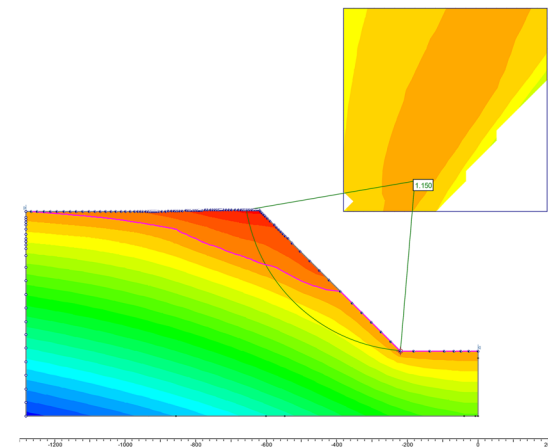
(b) Stability analysis diagram of safety factor of M-P method for section C2 under 45 ° stress I

(c) Stability analysis diagram of safety factor of simplified Bishop method for section C2 under 45 ° stress II

(d) Stability analysis diagram of safety factor of M-P method for section C2 under 45 ° stress II

(e) Stability analysis diagram of safety factor of simplified Bishop method for section C2 under 45 ° stress III

(f) Stability analysis diagram of safety factor of M-P method for section C2 under 45 ° stress III

Fig. 7 stability analysis diagram of C2 safety factor of section

(g) Stability analysis diagram of safety factor of simplified Bishop method for section C2 under 45 ° stress IV
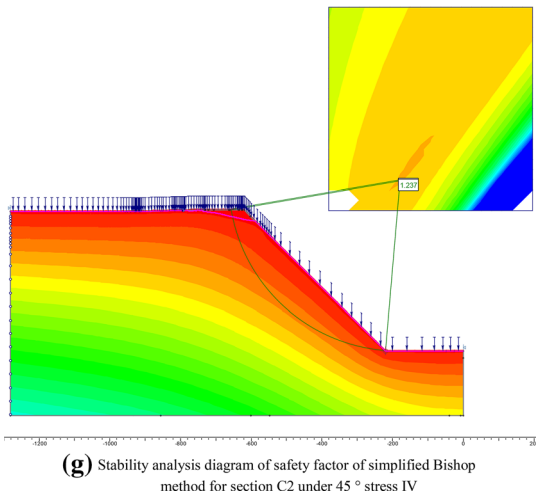
Fig. 7 continued

Self weight + groundwater + rainfall: [k] = 1.10.

If the calculated safety factor of the profile is $K >$ [k], it is stable. If $1 < K < $ [K], it is basically stable. if $K < 1$, it is unstable.

4 Analysis of Calculation Results

4.1 Preliminary Design Slope

The slope stability of 12 analysis sections is analyzed, and the design slope stability is evaluated according to the analysis results. The overall stability of the designed slope is analyzed according to four working conditions, and the analysis and calculation results are shown in Table 5. The typical stability analysis diagram of section B3 is shown in Fig. 6.

The analysis and calculation results in Table 6 show that the safety factor of the designed slope can meet the requirements of the allowable safety factor of the slope due to the slow overall slope angle, and has a large safety reserve. Therefore, it is necessary to optimize and adjust the end boundary of open-pit in K mine.

4.2 Optimization Design

In the form of one side slope, four kinds of stress conditions and overall stability analysis under different slope angles are carried out for 12 sections to determine the reasonable slope angle of each section,

that is, the most dangerous section of each section meets the maximum slope angle of the allowable safety factor. The typical C2 profile stability analysis results are shown in Fig. 7.

The optimal slope angle calculated finally is shown in Table 7, and the following conclusions are obtained based on the analysis results.

(1) Sections A1, B1, C2 and D1 meet the maximum overall slope angle of the allowable safety factor. Therefore, the reasonable slope angle of each zone is determined by the analysis results of these sections.

(2) With the increase of slope angle, the safety factor of slope decreases gradually.

(3) The influence of artificial blasting vibration on the slope stability is that the safety factor is reduced by $12.55\% \sim 14.54\%$ by using the simplified Bishop analysis method. The influence of natural VIII degree earthquake on slope stability is that the safety factor is reduced by $16.37\% \sim 22.05\%$. The influence of rainfall on slope stability is that the safety factor is reduced by $9.07\% \sim 16.19\%$. The influence of artificial blasting vibration on slope stability is that the safety factor is reduced by $12.55\% \sim 14.41\%$ by using M-P analysis method. The influence of natural VIII degree earthquake on slope stability is that the safety factor is reduced by $16.21\% \sim 21.79\%$. The influence of rainfall on the slope stability is that the safety factor is reduced by $9.24\% \sim 15.93\%$.

(4) According to the analysis results of the overall stability of the slope under four stress conditions and different slope angles of each section, the following slope angles can be used in different engineering geological divisions to ensure the stability of the slope, area $A \leq 46°$, area $B \leq 44°$, area $C \leq 45°$, area $D \leq 50°$ (see Table 6).

5 Numerical Simulation

5.1 Model Establishment

Three software coupling technologies, 3DMINE, MIDAS-GTS/NX and RHINO, are used in this numerical model. 3DMine has strong functions of line processing, triangulation and entity segmentation. 3D mine software is used to build the lithologic geological model of K mine in Myanmar. MIDAS-GTS/NX has a variety of advanced functions to build a set model. The terrain generator which simulates real

terrain can automatically read contour data to generate terrain and surface. It has a variety of constitutive models and provides user-defined constitutive interface. There are many kinds of grid generation methods, such as automatic grid generation, mapping grid generation and advanced grid generation. MIDAS-GTS/NX model is adopted for the design
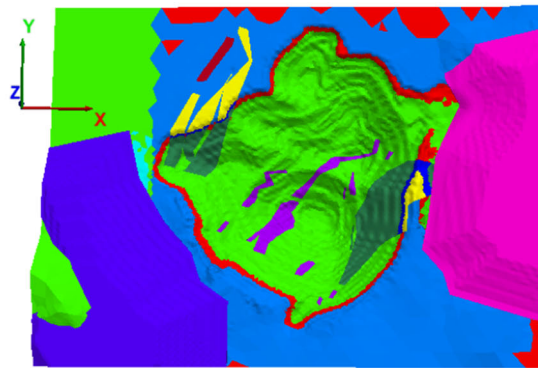
Table. 7 Basic information of FLAC3D modeling

Model	A	B
Range	x = 29715 m~32235 m (2520 m in total, east–west direction of the mining area)	
	y = 66852 m~68649 m (1797 m in total, north–south direction of the mining area)	
	Z is from 80 m to surface	
Elements	2,452,022	2,158,921
Nodes	1,852,644	1,698,575

(a) A model
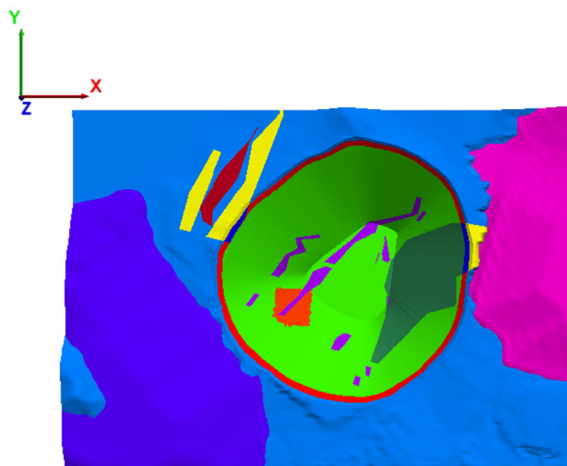
(b) B model

Fig. 8 FLAC3D model of A and B models

(a) A model section
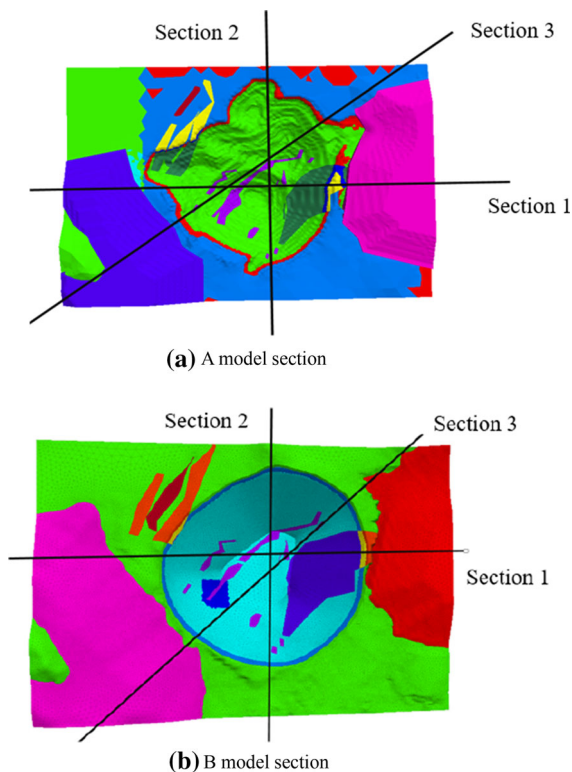

(b) B model section

Fig. 9 Location of a and B model sections

boundary model, and FLAC3D analysis and calculation are imported after grid division.

This model mainly analyzes the stability of the designed slope and the optimized slope. Design model refers to the final boundary slope of design. The optimization model refers to the recommended slope angle parameters after slope research. The slope angle selection of the optimized slope parameter is to establish a slope model according to the slope angle recommended in Table 5. The numerical analysis model of open-pit slope of K mine generated in FLAC3D is shown in Fig. 8. The selected positions of A and B model sections are shown in Fig. 9, and different colors in the figure indicate different lithology.

In the stability analysis of K mine slope, two situations are considered.

(1) Design slope.

The stability of the preliminary design slope is recorded as model A.

(2) Optimized slope.

The slope stability after the optimized slope angle is recorded as model B.

In the A and B models, boundary conditions and free surfaces are limited. Therefore, on the plane of X = 29715 m and 32235 m, all nodes are fixed in X direction. All nodes on the plane of y = 66852 m and 68649 m are fixed in Y direction. All nodes in Z = 80 m plane are fixed in X, Y and Z directions. The surface is free surface. The initial stress field is generated according to the self-weight stress field. Mohr Coulomb failure criterion is adopted as yield criterion.

5.2 Analysis of Simulation Results

Figure 10 is a cloud chart of safety factor and shear strain increment of model a as a whole and section, from which the following two conclusions can be drawn.

(1) The minimum safety factor of model a is 1.51, which is greater than the allowable safety factor of 1.25. The model is in a stable state.

(2) The larger increment of shear strain of model a is located in the moderately weathered and strongly weathered rocks in area A and B. The potential failure mode of the model is mainly "circular arc sliding". The safety factor of the model is high and it is stable.

Figure 11 shows the cloud chart of safety factor and shear strain increment of the whole and section of model B, from which the following two conclusions can be drawn.

(1) The minimum safety factor of model B is 1.43, which is greater than the allowable safety factor of 1.25. The model is in a stable state.

(2) The maximum increment of shear strain of model B is located near the free face of the slope within the range of waste dump in area A and area B, and the potential failure mode of model B is mainly "circular arc sliding".

6 Conclusions

In order to obtain the design slope stability of K mine open-pit in Myanmar, limit equilibrium analysis method and three-dimensional numerical simulation are used to carry out the study on the slope stability analysis. The following conclusions are obtained.
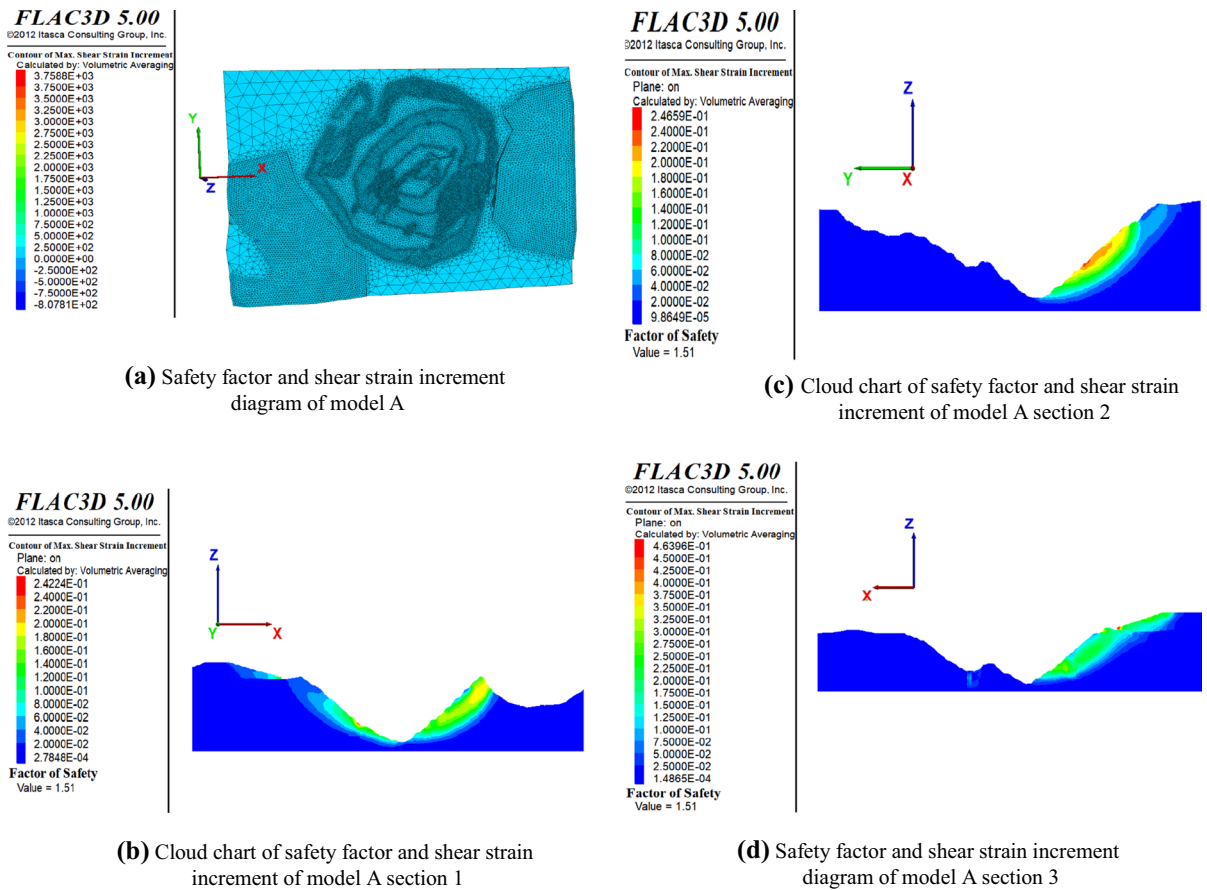
(a) Safety factor and shear strain increment diagram of model A

(c) Cloud chart of safety factor and shear strain increment of model A section 2

(b) Cloud chart of safety factor and shear strain increment of model A section 1

(d) Safety factor and shear strain increment diagram of model A section 3

Fig. 10 Cloud chart of safety factor and shear strain increment of model A

(1) The safety factor of the designed slope is greater than the allowable safety factor through the limit equilibrium analysis, which belongs to the stable slope, and some zones can be optimized for design.

(2) Through three-dimensional numerical analysis, the design slope and the optimized slope are both stable. The area with large deformation of the optimized slope is mainly concentrated above the 562 m level of moderately weathered pyroclastic rock in area a and above the 560 m level of moderately weathered rock in the scope of dumping in area B. The results of calculation are basically consistent with those of limit equilibrium analysis.

(3) Compared with the designed slope, the potential sliding surface position of the optimized slope is lower, and the safety factor is smaller, but larger than the allowable safety factor, which belongs to the stable slope. The shape of the sliding surface of the whole slope is nearly circular arc, so the sliding mode of the slope is circular arc sliding.
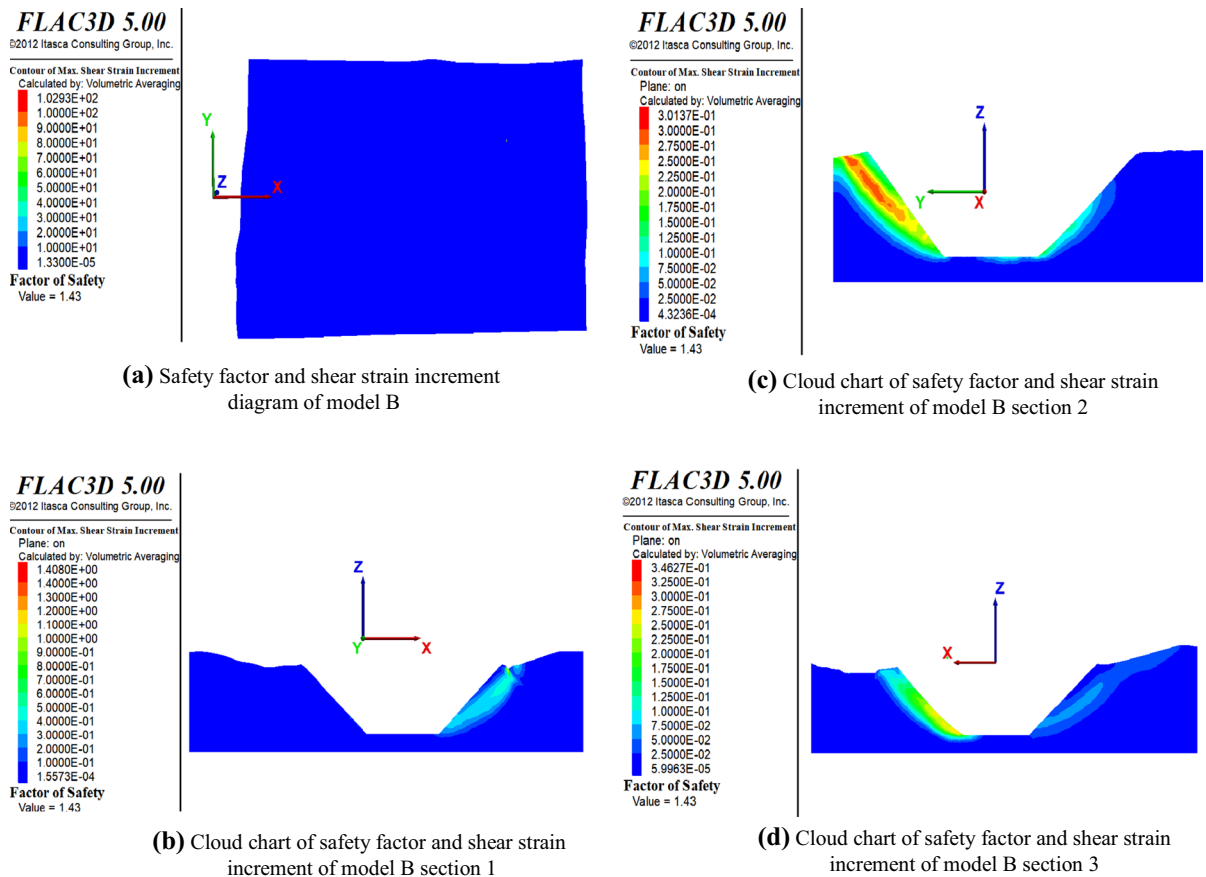
(a) Safety factor and shear strain increment
diagram of model B

(c) Cloud chart of safety factor and shear strain
increment of model B section 2

(b) Cloud chart of safety factor and shear strain
increment of model B section 1

(d) Cloud chart of safety factor and shear strain
increment of model B section 3

Fig. 11 Cloud chart of safety factor and shear strain increment of model B

(4) According to the comprehensive analysis results of the open-pit slope of K mine, considering the influence of various favorable and unfavorable factors on the slope stability, the reasonable slope angle of different engineering geological divisions of the open-pit slope of K mine is determined. The overall slope angle of area A is $\leq 46°$. The overall slope angle of area B is $\leq 44°$. The overall slope angle of area C is $\leq 45°$. The overall slope angle of area D is $\leq 50°$.

References

Chen Z, Mi H, Wang X (2001) A three-dimensional limit equilibrium method for slope stability analysis [J]. Chin J Geotech Eng 23(5):524–529

Cao L, Li H, Wang Z, et al. Deformation failure mechanism and stability of high and steep slope in open-pit mine [J].J Liaoning Tech Univ (Nat Sci), 2018,37(1):7–13.

Duncan JM, Wright SG (1980) The accuracy of equilibrium methods of slope stability analysis [J]. Eng Geol 16(12):5–17

Deng DP, Liliang L (2012) Analysis of slope stability and research of calculation method under horizontal slice method[J]. Rock Soil Mechan 33(10):3179–3188

Guan X, Wang X, Nie Q et al (2018) Stability analysis and parameters optimization of an open-pit slope[J]. Safety Coal Mines 49(5):71–74

Liu-qing H, Xibing L, Shiyou W (2011) The stability research of slope and its developing trend[J]. Mining Res Dev 20(5):7–8

Hovland HJ (1977) Three-dimensional slope stability analysis method [J]. J Geotech Environ Eng 103(9):971–986

Hungr O (1987) An extension of Bishop's simplified method of slope stability analysis to three-dimensions [J]. Geotechnique 37:113–117

Huang CC, Tsai CC (2000) New method for 3D and asymmetric slope stability analysis [J]. J Geotech Environ Eng 126(10):917–927

Han X, Lu C (2018) Structural optimization and stability study on bedding high slope with medium angle[J]. Modern Mining 4:174–177

Jyant K, Pijush S (2006) Stability determination for layered soil slopes using the upper bound limit analysis[J]. Geotech Geol Eng 24(6):1803–1819

Liu X, Ma Z, Huang Z et al (2017) Optimization and stability analysis of slope in Luming Molybdenum Mine based on the limit equilibrium method[J]. Non-Ferrous Metals (Mine Part) 69(03):64–67

Pan Y, Ruan Y, Huang Y (2017) Study on the slope treatment of open-pit mine in alpine area[J]. Mining Res Dev 37(7):31–34

Wang D, Cao L, Song Z (2009) Study on slope stability in combine mining based on RFPA-SRM[J]. J Hefei Univ Technol (Nat Sci) 10:1562–1565

Yang T, Zhang F, Yu Q et al (2011) Research situation of open-pit mining high and steep slope stability and its developing trend[J]. Rock Soil Mech 32(5):1437–1472

Zou P, Li A, Liu Z et al (2016) Optimization study on the structure parameter of slope in an open-pit waste dump[J]. Mining Res Dev 36(9):46–49